**Individual variation in brain microstructural-cognition relationships in aging**

Raihaan Patel[a,b*], Clare E. Mackay[c,d], Michelle G. Jansen[e], Gabriel A. Devenyi[a,f], M. Clare O'Donoghue[c,d], Mika Kivimäki[g], Archana Singh-Manoux[g,h], Enikő Zsoldos[c,d], Klaus P. Ebmeier[c], M. Mallar Chakravarty[a,b,f,1*], Sana Suri[c,d,1*]

[*]Corresponding author, [1]Joint senior authorship

[a]Computational Brain Anatomy Laboratory, Cerebral Imaging Centre, Douglas Mental Health University Institute, Verdun, Québec H4H 1R3, Canada

[b]Department of Biological and Biomedical Engineering, McGill University, Montréal, Québec H3A 2B4, Canada

[c]Department of Psychiatry, Warneford Hospital, University of Oxford, OX3 7JX, Oxford, United Kingdom

[d]Oxford Centre for Human Brain Activity, Wellcome Centre for Integrative Neuroimaging, University of Oxford, OX3 7JX, Oxford, United Kingdom

[e]Donders Centre for Cognition, Donders Institute for Brain, Cognition and Behaviour, Radboud University, Nijmegen, the Netherlands

[f]Department of Psychiatry, McGill University, Montréal, Québec H3A 1A1, Canada

[g]Department of Epidemiology and Public Health, University College London, WC1E 6BT London, United Kingdom

[h] Université de Paris, Inserm U1153, Epidemiology of Ageing and Neurodegenerative diseases, 75010 20 Paris, France

# Abstract

The sources of inter- and intra-individual variability in age-related cognitive decline remain poorly understood. We examined the association between 20-year trajectories of cognitive decline and multimodal brain microstructure and morphology in older age. We used the Whitehall II Study, an extensively characterised cohort with 3T brain magnetic resonance images acquired at older age (mean age = 69.52± 4.9) and 5 repeated cognitive performance assessments between mid-life (mean age = 53.2 ±4.9 years) and late-life (mean age = 67.7 ±4.9). Using non-negative matrix factorization, we identified 10 brain microstructural components integrating cortical thickness, surface area, fractional anisotropy, and mean and radial diffusivities. We observed two latent variables describing distinct brain-cognition associations. The first describes variations in 5 microstructural components associated with low mid-life performance across multiple cognitive domains, decline in reasoning, but maintenance of fluency abilities. The second describes variations in 6 microstructural components associated with low mid-life performance in fluency and memory, but retention of multiple abilities. Expression of latent variables predicts future cognition 3.2 years later (mean age = 70.87 ±4.9). This data-driven approach highlights brain-cognition relationships wherein individuals express both decline *and* maintenance in function across cognitive domains and in brain structural features.

# 1.0 Introduction

Cognitive decline is a well-established aspect of the aging process. Age-related impairments which impact everyday functioning have been reported across a range of cognitive domains (Salthouse 2010; Tucker-Drob 2011a). However, significant inter-individual variability has also been observed across cognitive domains including memory, spatial functioning, processing speed and reasoning. While some individuals experience accelerated rates of deterioration, others experience a relative maintenance of cognitive functioning into old age (Wilson et al. 2002; Tucker-Drob and Salthouse 2011; Pudas et al. 2013). Even within the same individual, some cognitive domains may remain intact whereas other domains are more vulnerable to decline (Tucker-Drob 2011b). It is unclear whether this intra- and inter-individual variation arises from underlying changes already present in early-to-mid life, or if they are established in older age. Improving our understanding of the sources of this variability is an important step in understanding aging-related changes in cognition.

Numerous magnetic resonance imaging (MRI) studies have suggested that inter-individual variation in cognitive function may be partially explained by differences in brain structure, be it through differences in neurobiology at a given time (brain reserve) or in preservation of brain morphology changes during ageing over time (brain maintenance), (Stern et al. 2020). MRI provides macro- and microstructural measures such as volume, thickness, surface area, diffusivity and fractional anisotropy, each of which convey complementary information about the local morphology, axonal density, organization and myelination of the cerebral cortex (Tardif et al. 2016; Lerch et al. 2017). In healthy aging, these techniques have demonstrated widespread age-related degeneration of brain structure, namely decreases in overall brain volume (Hedman et al. 2012), cortical thickness (Fjell et al. 2014; Shaw et al. 2016; Lowe et al. 2019), and fractional anisotropy as well as increases in diffusivity (Marner et al. 2003; Bartzokis 2004; Lebel et al. 2012; Tardif et al. 2016). They have also provided evidence for a brain-cognition link in aging, for example by previously established associations between episodic memory performance with volumes and diffusivity of the medial temporal lobe (Raz and Rodrigue 2006; Philippi et al. 2016; Reas et al. 2018; Schneider et al. 2019), and between decline in executive functioning and widespread grey matter atrophy (Schneider et al. 2019).

However, most studies to date have considered these micro- and macro-structural MRI metrics individually, without considering the complementary information multiple metrics provide on brain structure, or their potential overlap and interdependencies. Moreover, most studies have considered a priori definitions of cognitive decline. Previous approaches investigating brain-cognition relationships have defined subject groupings based on cognitive trajectories and then assessed group differences in brain structure (Persson et al. 2006; Schneider et al. 2019). For example, individuals have been broadly categorised as cognitive “maintainers”, or “decliners” (Josefsson et al. 2012). A common strategy is to categorize the most severe decliners and compare them to the rest of a cohort (Schneider et al. 2019). This approach involves arbitrary cut-offs, and may be biased by the extremes of the decliner-maintenance dimension, neglecting individuals demonstrating neither sharp decline nor strong maintenance (Persson et al. 2012). Furthermore, broad categorisations of maintainers/decliners may also ignore intra-individual

heterogeneity and the differential impact of age across cognitive domains (Rönnlund et al. 2005; Park and Reuter-Lorenz 2009; Goh et al. 2012).

This study builds on previous work in two important ways. First, we integrate multiple MRI based indices of cortical microstructure. Incorporating data from multiple MRI modalities is useful as each conveys complementary information, such that the resulting multimodal assessments query a wider range of biological phenomena (Tardif et al. 2016). This approach has enabled fine grained assessments of the cerebral cortex. Glasser et al., for example, incorporated data from structural and functional MRI to delineate a novel parcellation of the cortex, including the identification of de novo areas distinguishable as a result of this strategy (Glasser et al. 2016). Seidlitz et al. integrated multimodal MRI indices of cortical microstructure to identify morphometric networks, such that areas of the cortex displaying morphometric similarity shared cytoarchitectonic and transcriptional features (Seidlitz et al. 2018). These findings demonstrate the specificity of associations demonstrated using multimodal MRI. Modelling shared covariance across MRI metrics, as opposed to separately analysing each piece of information, allows for a more comprehensive assessment of differences across subjects (Groves et al. 2012). To this end, we expand previous work from our group on multi-modal data-driven parcellation of the hippocampus using non-negative matrix factorization (NMF), and extend this methodology to facilitate integration of multiple modalities into a single analytical framework (Patel et al. 2020) (Patel et al. 2020). Applied to MRI data, NMF highlights regions of the brain in which shared patterns of microstructural variation occur. (Lee and Seung 1999; Sotiras et al. 2015; Patel et al. 2020).

Second, we explore individual differences in brain-cognition relationships without *a priori* designations of cognitive trajectories. We instead use a data-driven approach to probe the relationships between brain microstructure and cognition. We employ partial least squares (PLS), a multivariate technique used to relate two sets of variables together (McIntosh and Lobaugh 2004), to identify covarying relationships between brain microstructure and cognitive performance in a data-driven fashion. This approach sidesteps the need for *a priori* definitions and enables identification of dimensions along which subject-specific brain-cognition relationships exist, instead of distinct decline/maintenance categorizations. Importantly, we then assess biological significance of the identified patterns by exploring how individual variation in these dimensions predicts future cognitive performance.

In this study we analyse data from the Whitehall II cohort, a unique and comprehensive longitudinal dataset which enables study of the relationship between mid- and late-life features. This ongoing study was established in 1985 at University College London and initially included 10,308 British civil servants (Marmot and Brunner 2005). Longitudinal follow-up occurred at multiple timepoints (defined throughout as Waves). We analyse data collected between 1997 and 2016, collected roughly every five years at Wave 5 (1997-1999), 7 (2002-2004), 9 (2007-2009), 11 (2012-2013), and 12 (2015-2016). At each Wave, information on social, cognitive, and biological data was collected, resulting in a unique source of information to study aging. Eight hundred individuals from Wave 11 were randomly selected to participate in the Whitehall II Imaging sub-study (Imaging Wave, 2012-16) in which structural, diffusion, and functional MRI was collected (Filippini et al. 2014). In this work, we leverage this unique dataset along with multivariate techniques to identify brain-cognition modes of covariance by relating multimodal MRI measures of late-life brain microstructure with cognitive trajectories from mid- to

late-life. We then examine the biological significance of the brain-cognition relationships by testing their association with future cognitive performance.

# 2.0 Methods

Using the comprehensive lifespan data from the Whitehall II Imaging sub-study (Figure 1A), we analyse longitudinal cognitive trajectories across multiple domains and assess their relationship with late-life cortical microstructure using surface area (SA), cortical thickness (CT), mean diffusivity (MD), fractional anisotropy (FA) and radial diffusivity (RD). Across multiple microstructural MRI indices, we model shared covariance using NMF. We use linear mixed effects modeling to extract subject specific indices of baseline performance and change in performance across multiple cognitive tests during a period of 20 years. We then use partial least squares (PLS) to identify distinct patterns of covariance between microstructure and longitudinal cognitive performance, which we term brain-cognition latent variables (Figure 1B) (McIntosh and Lobaugh 2004; McIntosh and Mišić 2013). Finally, we use each individual's expression of the identified latent variables to predict cognitive function at a follow-up timepoint, approximately 3.2 years after the MRI scan (Wave 12) (Figure 1C).

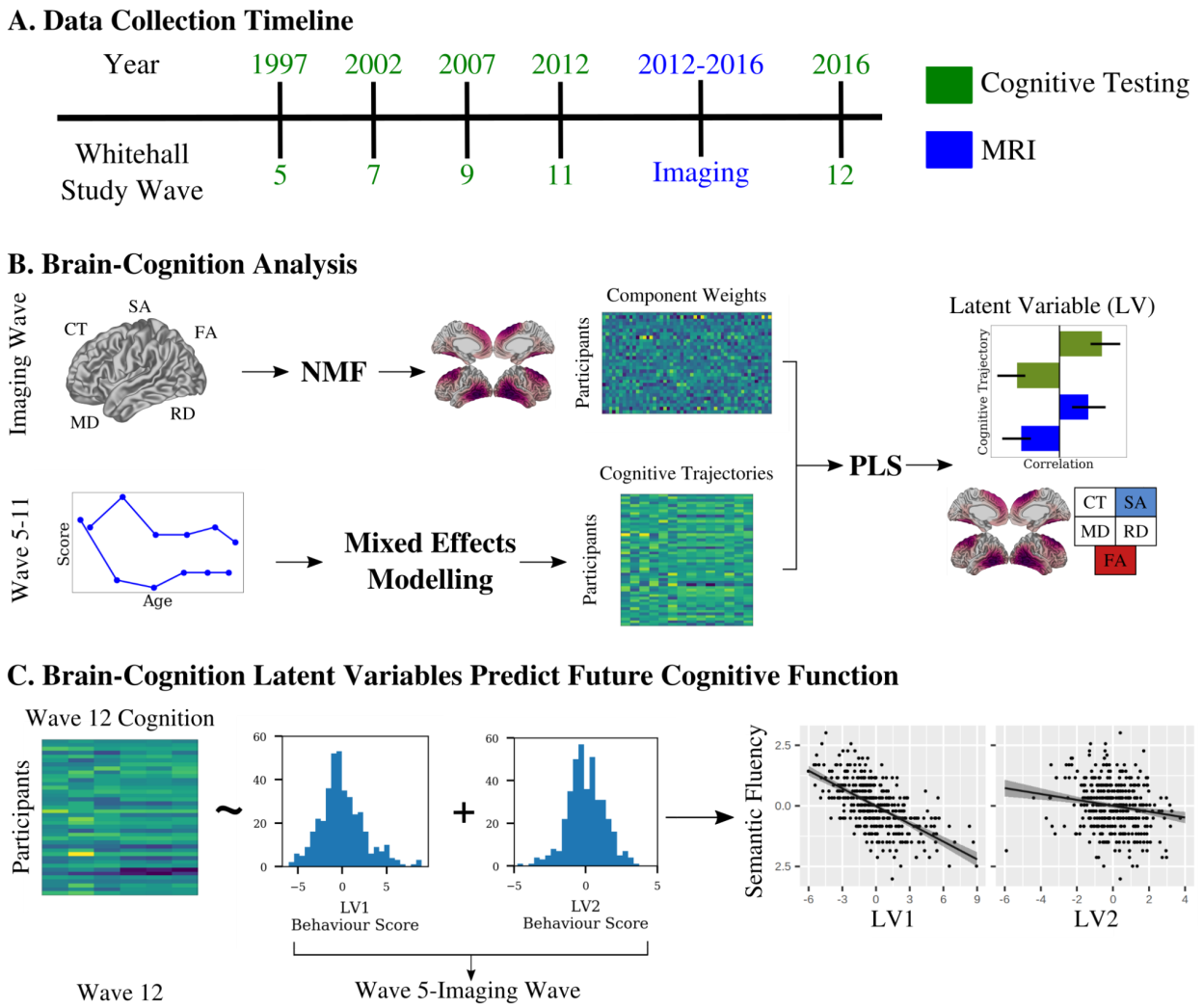


Figure 1. **Identifying microstructural-cognition relationships in aging using data-driven techniques.** A) We analysed data from the Whitehall II Imaging Sub-Study. Participants were tested across multiple cognitive domains at ~5-year intervals since 1997, with structural and diffusion MRI collected between Waves 11 and 12. B) We applied non-negative matrix factorization (NMF) to five metrics of cortical morphology: cortical thickness (CT), surface area (SA), fractional anisotropy (FA), and mean and radial diffusivity (MD, RD) to identify patterns of variance. Using cognitive data from Wave 5-11, we applied mixed effects modelling to identify intercept and slope measurements for each individual across a range of cognitive tests during the 20-year period. We then used a partial least squares (PLS) analysis to identify brain-cognition latent variables describing covariance between longitudinal cognitive trajectories and late life cortical morphology. C) We related expression of the brain-cognition latent variables to future cognition to show the identified brain-cognition latent variables predict future performance in two distinct ways.

## 2.1 Sample

We used data from the Whitehall II Imaging Sub-Study (Filippini et al. 2014), a random sample of 800 individuals from the Whitehall II Study of British civil servants, of which 775 received an MRI scan (Marmot and Brunner 2005). These individuals have been assessed longitudinally since 1985 across a total of 12 waves thus far. Cognitive performance was assessed at 5 timepoints at University College London: Wave 5 (1997-1999), Wave 7 (2002-2004), Wave 9 (2007-2009), Wave 11 (2012-2013), and Wave 12 (2015-2016). Structural and diffusion weighted magnetic resonance imaging (MRI) was conducted at the University of Oxford between 2012-2016 (Imaging Wave, Figure 1). Montreal Cognitive Assessment (MOCA) was also conducted at the Imaging Wave to be used as a covariate during subsequent analyses.

## 2.2 MRI Acquisition

MRI data was acquired on one of two scanners - a 3T Siemens Magnetom Verio (Erlangen, Germany) (n=552) or a 3T Siemens Magnetom Prisma scanner (Erlangen, Germany) (n=223) at the FMRIB Centre in the Wellcome Centre for Integrative Neuroimaging (WIN), Oxford. T1 weighted images were acquired using a Multi-Echo MPRAGE (MEMPR) sequence (1mm$^3$, TR = 2530ms, TE = 1.79/3.65/5.51/7.37ms) on the Verio scanner and a closely-matched MPRAGE sequence on the Prisma scanner (1mm$^3$, TR=1900ms, TE=3.97ms). Diffusion weighted imaging (DWI) was acquired with an identical sequence across both scanners, using monopolar diffusion encoding gradients with parallel imaging at 2mm isotropic (60 directions, b=1500s/mm$^2$). Detailed acquisition descriptions have been described elsewhere (Filippini et al. 2014).

## 2.3 Obtaining Brain Microstructural Metrics

T1w images were preprocessed using the minc-bpipe-library (https://github.com/CoBrALab/minc-bpipe-library), including bias field correction (Tustison et al. 2010), adaptive non-local means denoising (Manjón et al. 2010), head masking and brain extraction (Eskildsen et al. 2012) The resulting bias field corrected, head-masked images and brain masks of each subject were input into the CIVET algorithm (Lerch and Evans 2005; Ad-Dab'bagh et al. 2006) (version 2.1.0) in order to obtain cortical mid-surfaces and vertex wise measures of cortical thickness (CT) and surface area (SA), describing CT and SA estimates at a total of 81924 points across the cortical mid-surface. Vertex wise CT and SA were blurred using 30 mm and 40 mm geodesic surface kernel, respectively. We masked out 4802 vertices located along the left and right midline as CT and SA estimates in this region are unreliable or nonexistent, resulting in a total of 77122 vertices valid for analysis. CIVET outputs were quality controlled for registration quality, grey/white matter classification accuracy, and surface abnormalities by one of the authors (RP).

DWI data were preprocessed using the FMRIB's diffusion toolbox (FDT), with a generative model approach to estimate and correct for distortions due to susceptibility, eddy currents, and head motion simultaneously. DTIFit (https://fsl.fmrib.ox.ac.uk/fsl/fslwiki/FDT) was used to generate maps of MD, FA,

and RD for each subject. For each subject, MD, FA, and RD images were registered to their T1w image using a multispectral affine registration. The resulting transformations were used to transform the cortical mid-surface to the DWI space. Vertex wise estimates of each of MD, FA, and RD were obtained using the transformed surfaces to correspond with the previously obtained vertex wise CT and SA measures. Like CT and SA data, left and right midline data was masked out resulting in a total of 77122 data points for each of MD, FA, and RD.

## 2.4 Identifying Components using Non-negative Matrix Factorization

We used non-negative matrix factorization (NMF) to identify microstructural components, motivated by previous work from our group deriving a multi-modal microstructural parcellation of the human hippocampus (Patel et al. 2020). NMF is a matrix decomposition technique which decomposes an input matrix into two matrices containing components and weights, respectively. In the context of this analysis, NMF identifies regions of the brain where inter-individual microstructural variation is observed (spatial components) as well as each individual's microstructural profile in a given component (subject weightings). Together, these outputs localize individual variability to specific brain regions in a data-driven manner. As the name suggests, NMF requires non negativity in both inputs and outputs, leading to an additive parts-based representation (Lee and Seung 1999). Given an input matrix of dimensions m x n, NMF outputs a component matrix W (m x k), and a weight matrix H (k x n). The number of components, k, is defined by the user.

In this implementation, the NMF input matrix is constructed by stacking the vertex x subject matrices of each microstructural metric together, forming a matrix with 77122 rows and 1990 columns (77122 vertices, 398 subjects * 5 metrics = 1990 columns). At each vertex, and for each microstructural metric, we model out the effect of scanner using linear regression and then perform z-scoring on the residuals. This minimizes any local scanner bias, and spatially normalizes each measure. The resulting matrices are then stacked side by side to form a matrix containing z-scored and residualized data across all microstructural metrics. This matrix is shifted by its minimum value to create a non-negative input matrix for NMF. We used sklearn (version 0.23.1) to implement NMF with a non-negative singular value decomposition initialization to improve sparsity (Boutsidis and Gallopoulos 2008). Number of components was selected through a split half stability analysis and a balance of spatial stability and model reconstruction accuracy (Patel et al. 2020).

## 2.5 Cognitive Function Trajectories

We used 5 tests to measure cognitive performance. These include semantic fluency (in one minute, recall as many animals as possible), lexical fluency (in one minute, recall as many words starting with "S" as possible), short term memory (20 word free recall, recall within two minutes), inductive reasoning through the Alice-Heim 4-I (AH4) test (Heim 1970), and vocabulary using the Mill Hill test (Raven 1958; Singh-Manoux et al. 2012). We included the total AH4 score (inductive reasoning) as well as mathematical and verbal reasoning sub scores, giving a total of 7 cognitive scores. For each score, a linear mixed effects model was performed with an interaction of baseline age and time since baseline as a fixed effect, a random slope of time since baseline, and random intercept for each subject (1).

$$TestScore \sim Baseline\ Age * Time + (1 + Time|Subject) \quad (1)$$

Models were implemented in R (version 3.6.3) using the nlme (version 3.1-149) package and implemented continuous autoregressive moving-average correlation structure to consider correlations between repeated measures on the same individual. Importantly, cognitive test data prior to the MRI time point (Wave 5-11 but excluding Wave 12) was included in the linear mixed effects modelling. For each model we extracted subject-specific intercepts, as well as the slope (i.e. coefficient) of the time variable (using the R coef() function). These values are a summation of the overall fixed effects and subject-specific random effects (De Jager et al. 2012), thus representing individual differences in modelled baseline performance (intercept) and impact of time (slope).

## 2.6 Partial Least Squares

To investigate microstructural cognition relationships, we performed a brain-cognition partial least squares analysis (PLS). PLS is a multivariate technique which aims to maximize the covariance between two sets of variables (McIntosh and Lobaugh 2004; Krishnan et al. 2011; McIntosh and Mišić 2013). In this implementation, brain variables correspond to a 398 x 50 matrix containing NMF weightings of each subject within each of 10 components, for each of 5 microstructure metrics. Cognitive data corresponds to a 398 X 14 matrix containing intercept and slope measures for each subject, for each of the 7 cognitive test scores. PLS outputs latent variables (LV), each describing a pattern of covariance between microstructural NMF weights and cognitive intercepts and slopes. Each brain-cognition LV includes a singular value used to measure the proportion of total covariance explained. Statistical significance of an LV is assessed using permutation testing (n=10000), which develops a null distribution of singular values from which a non parametric p-value of each singular value in the original, non permuted data is computed. Bootstrap resampling is used to generate distributions of the singular vector weights of each brain and cognition variable, which enables identification of a confidence interval associated with each brain and cognition variables contribution to a given LV (McIntosh and Lobaugh 2004; Krishnan et al. 2011; Zeighami et al. 2017; Nordin et al. 2018).

## 2.7 Predicting Future Cognition Using Brain-Cognition Latent Variables

To further investigate the biological significance of the LVs, we performed linear models to examine the relationship between LV behaviour scores and future cognitive performance (i.e. cognitive scores at Wave 12, 3.2 years after the MRI scan. For each cognitive score, we modelled Wave 12 performance as a function of the interaction between LV1 and LV2 behaviour scores while covarying for age, sex and years of education using a model of the form

$$Wave12TestScore \sim LV1 * LV2 + Age + Sex + Education \quad (2)$$

Where LV1 and LV2 terms represent behaviour scores of each individual in a given LV. We performed the above model for 6 of the 7 test scores used in the PLS analysis described in section 2.6 (Mill Hill test was not conducted at Wave 12 and thus is not included in this analysis). Given the count nature and skew of cognitive test scores, a square root transformation followed by inverse normal transformation was applied

to these data prior to linear modelling. Terms of interest included the LV1, LV2 terms and their interaction, assessed at a bonferroni threshold of 0.0083 (0.05 / 6 tests). To complete our characterization of LV behaviour scores, we repeated this analysis using untransformed test score data and assessed relationships between LV behaviour scores and each of age, MOCA status, sex, and education at the Imaging Wave.

## 2.8 Data Availability

The study follows Medical Research Council data sharing policies (https://mrc.ukri.org/research/policies-and-guidance-for-researchers/data-sharing/). In accordance with these guidelines, data from the Whitehall II Study and the Imaging Sub-study are accessible via a formal application on the Dementias Platform UK portal (https://portal.dementiasplatform.uk/). Code used in this analysis is available at https://github.com/raihaan/micro-cog-nmf.

# 3.0 Results

## 3.1 Sample

The final analysis sample included 398 individuals who passed quality control for motion and cortical thickness processing, and had whole brain DWI available (mean age = 69.5 years ± 4.2, 92 females (23%), mean education years = 14.2 ± 3). Comparison of the analysis and initial samples is shown in Table 1. For further details on sample selection, see SI Methods and Figure S1.

**Table 1:** Demographic characteristics for the analysis and starting samples including mean and standard deviations for age, years of education, and MOCA score at the MRI Wave. Number of women, as well as number of individuals with MOCA score >=26, indicative of no major cognitive impairments, is shown.. Statistical tests (t-test or chi-squared) show no differences between the analysis sample and full starting sample.

| | **Analysis sample (N=398)** | **Starting sample (N=775)** | **Test Statistic** | ***p*** |
|---|---|---|---|---|
| Age (years) | 69.52± 4.9 | 69.81±5.19 | $t = 0.95$ | 0.35 |
| Education (years) | 15.84±3.54 | 15.72±3.53 | $t = -0.58$ | 0.57 |
| MOCA score | 27.29±2.23 | 27.18±2.26 | $t = -0.80$ | 0.42 |
| Women, N (%) | 92 (23.1%) | 150 (19.3%) | chi-squared $= 2.27$ | 0.13 |
| MOCA>=26, N (%) | 322 (80.9%) | 614 (79.2%) | chi-squared $= 0.46$ | 0.49 |

| | | | | |
|---|---|---|---|---|
| N (%) of participants scanned on Verio MRI scanner | 281 (70.6%) | 552 (71.2%) | chi-squared $= 0.49$ | 0.82 |

## 3.2 Non-negative matrix factorization identifies 10 stable microstructural components

NMF analysis was performed on an input matrix consisting of cortical measurements of all subjects CT, SA, MD, FA, and RD data.(Sotiras et al. 2015; Patel et al. 2020). Split half stability analysis (Patel et al. 2020) identified 10 components as a suitable balance between spatial stability and reconstruction error (see SI Methods and Figure S2). The 10 spatial components and associated weightings are displayed in Fig 2A and 2B, respectively. Each component identifies a group of vertices which share a covariance pattern for CT, SA, MD, FA, and RD. The components are largely bilateral and non-overlapping, and their regional descriptions and naming conventions are described below.

1. Component 1: (Fronto-Temporal) is localized in the superior frontal and posterior temporal regions.
2. Component 2: (Motor) is localized to primary and supplementary motor cortices, with some spread to adjacent posterior frontal and superior parietal regions.
3. Component 3: (Visual) is strongly localized in the medial and lateral occipital lobe, as well as the cingulate cortex and inferior temporal lobe.
4. Component 4: (Parietal) occupies most of the parietal cortex, with some spread to the lateral temporal regions.
5. Component 5: (Inferior Frontal) is most prominent in the inferior, medial frontal lobe, but also shows some presence in the inferior temporal lobe, anterior cingulate regions, and inferior lateral frontal lobe.
6. Component 6: (Anterior Frontal) occupies the anterior frontal regions as well as the temporal pole.
7. Component 7: (Cingulate) occupies much of the midline regions but with a strong preference to the cingulate cortex and shows some spread to insular cortices.
8. Component 8: (Postcentral) is heavily localized to the postcentral gyrus but shows considerable presence in the lateral inferior frontal lobe and superior temporal gyrus.
9. Component 9: (Right lateralized) is the only component showing a laterality effect, including bilateral medial parietal anterior temporal regions, but most prominent in right superior temporal and lateral inferior frontal regions.
10. Component 10: (Temporal Pole) is most prominent in the temporal pole, but also shows some presence in medial temporal and ventromedial frontal areas.

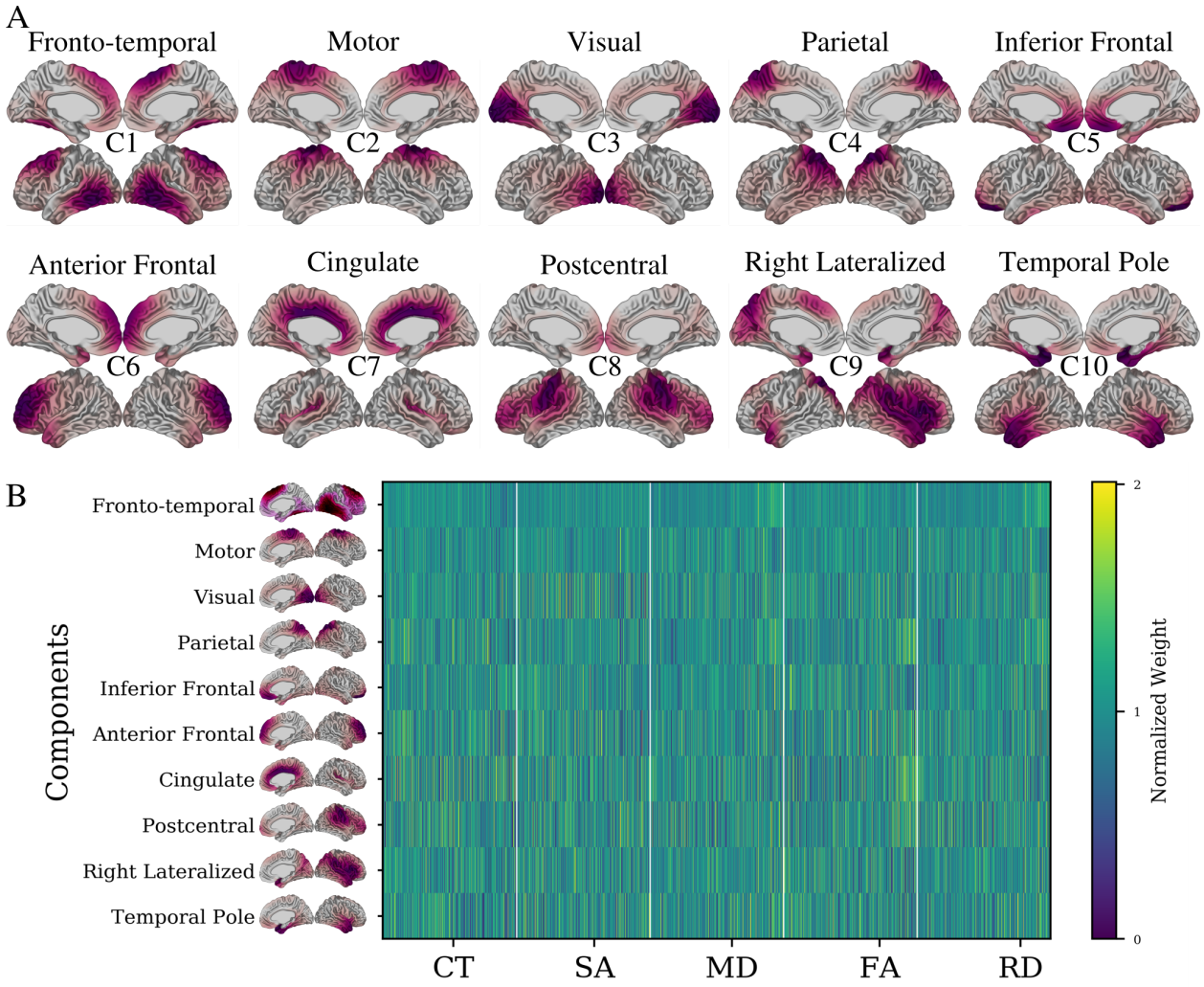


Figure 2. **10 microstructural components derived from the NMF decomposition.** A) Cortical mappings of each of the spatial patterns for each of the 10 components. For each component, lateral and medial views of both left and right hemispheres are shown. Components are identified using the putative descriptors from the main text (e.g., Fronto-temporal) as well as lettering at the centre of each set of surface views (e.g., C1). Red areas indicate vertices loading heavily onto a particular component (thresholded at 25% to max value). Each component identifies a selection of vertices sharing a microstructural variance pattern. Together, components cover the entire brain, are largely bilateral (with exception of component 9) and are not spatially overlapping. B) Subject-specific weightings associated with each of the displayed 10 components. Each row corresponds to a specific component's NMF weightings for each subject-metric combination, describing the CT, SA, MD, FA and RD patterns of each subject in each component. Together these two outputs describe the morphological patterns of each subject within each spatial component. Each element of the matrix is displayed as a fraction of its row mean, such that values below 0 indicate a below average weight for a given component and vice versa.

## 3.3 Specific Patterns of Cortical Morphology Relate to Baseline and Longitudinal Cognitive Function

We next related the variation in cortical microstructure captured by the NMF subject weightings to variability in cognitive performance over time. For each participant we derived the intercept and slope for the change in performance across each of seven cognitive tests: lexical and semantic fluency, short-term memory, verbal, mathematical and inductive reasoning, and vocabulary (SI Results Table S1). The intercept describes the estimated baseline (i.e., mid-life) performance while the slope describes the linear rate of change in performance over time (i.e., from mid-life to late-life). We performed a brain-cognition PLS with NMF component weightings as "brain" data and intercept and slope measurements as "cognition" data. PLS analysis identified two significant latent variables (LVs), explaining 56.9% and 19.7% of shared brain-cognitive covariance respectively. Each LV identifies a distinct pattern of longitudinal cognitive trajectories across the 20-year follow up that relate to patterns of late-life microstructural characteristics (Figure 3).

LV1 describes a pattern in which low baseline performance across all tests, accelerated 20-year decline in inductive, verbal, and mathematical reasoning abilities, but slow 20-year decline in verbal and semantic fluency are associated with global decreases in late-life SA, lower CT (cingulate/insular), lower FA (visual, temporal, right lateral), higher MD and RD (temporal pole), and paradoxically higher FA in posterior temporal and superior frontal regions. (Figure 3A, Table 2). LV2 describes a pattern in which low baseline performance in each of lexical fluency, semantic fluency, and short term memory, but slower decline in each of lexical fluency, semantic fluency, inductive reasoning, verbal reasoning, and numeric reasoning is associated with global increases in SA, higher CT and lower RD in the temporal pole, increased MD in inferior frontal, anterior frontal, and cingulate cortices, increased RD in motor, anterior frontal, and cingulate cortices, and decreased FA (anterior frontal, cingulate/insular) (Figure 3B, Table 2).

In summary, each brain-cognition LV described mixed patterns of cognitive decline and maintenance, as well as degeneration and preservation of cortical microstructure. This suggests that rather than cognitive decline being linked with uniform cortical degeneration, individuals display degrees of degeneration *and* preservation of cortical microstructure that is linked with decline *and* maintenance across diverse cognitive functions.

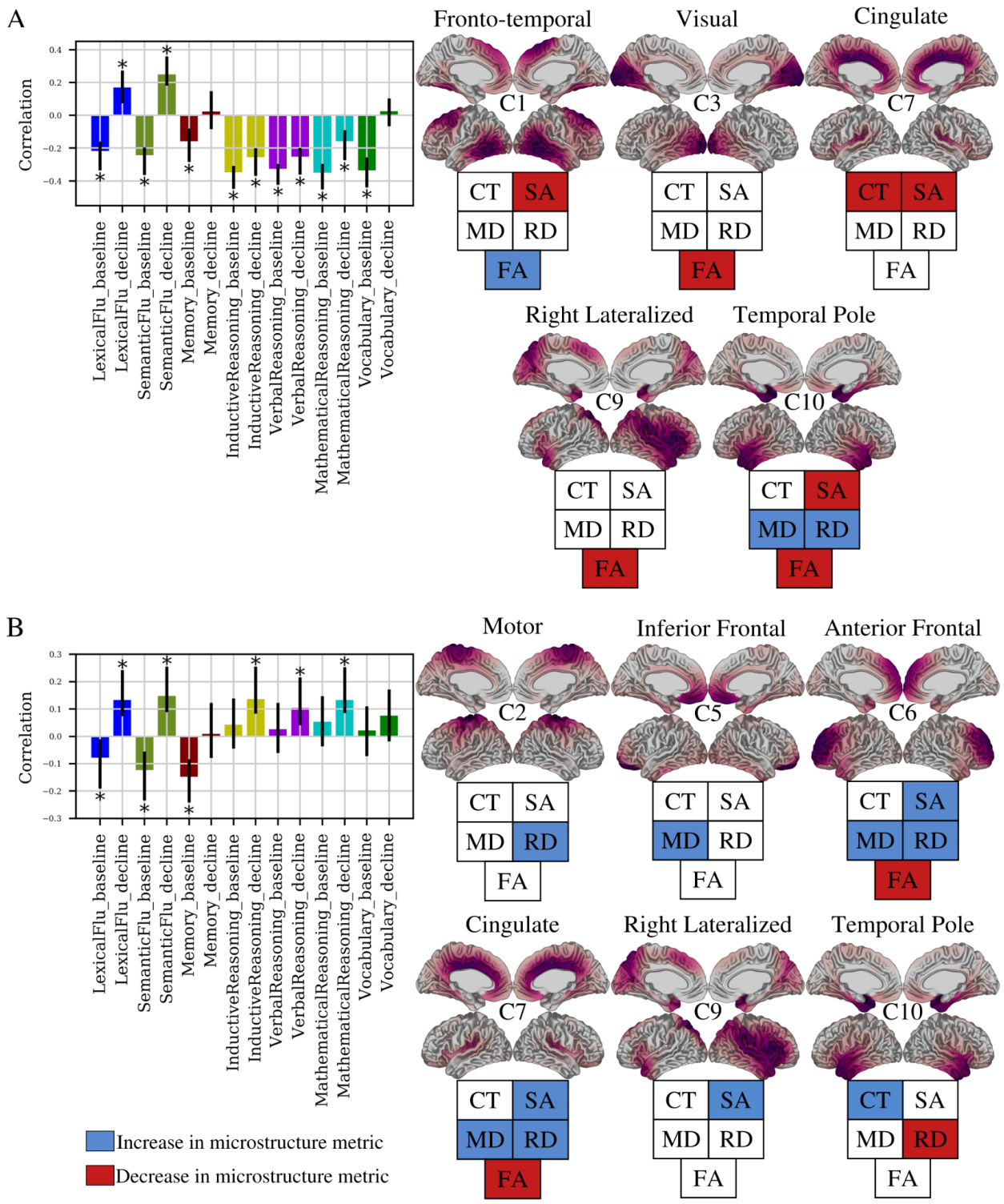


Figure 3: **Two brain-cognition latent variables identified by PLS**. PLS identified two (LV1: A, LV2: B) significant latent variables (p<0.05), each identifying a pattern of covariance between NMF weights and cognitive intercept and slopes. Bar plots describe contribution of cognitive variables. The y-axis denotes correlation of each cognitive variable in a LV. Error bars denote 95% confidence interval, only variables with non-zero confidence interval are described as contributing to a LV (marked with *). For each bar plot, cortical maps (right) show spatial

patterns of the components contributing to the LV. The fingerprint of each map describes whether a given metric is decreased (blue) or increased (red) in the spatial component in relation to the cognitive pattern shown in bar plots.

**Table 2:** Correlations of the contributing cognitive variables to each latent variable

| Brain-Cognition Latent Variable | Parameter | Cognitive Test | R [95% CI] |
|---|---|---|---|
| 1 | Intercept | Lexical Fluency | -0.22 [ -0.33 , -0.16 ] |
| | | Semantic Fluency | -0.24 [ -0.36 , -0.2 ] |
| | | Short Term Memory | -0.16 [ -0.28 , -0.09 ] |
| | | Inductive Reasoning | -0.35 [ -0.45 , -0.31 ] |
| | | Verbal Reasoning | -0.33 [ -0.42 , -03 ] |
| | | Mathematical Reasoning | -0.35 [ -0.45 , -0.3 ] |
| | | Vocabulary | -0.34 [ -0.44 , -0.26 ] |
| | Slope | Lexical Fluency | 0.17 [ 0.07 , 0.27 ] |
| | | Semantic Fluency | 0.25 [ 0.18 , 0.36 ] |
| | | Inductive Reasoning | -0.26 [ -0.37 , -0.2 ] |
| | | Verbal Reasoning | -0.25 [ -0.36 , -0.2 ] |
| | | Mathematical Reasoning | -0.16 [ -0.27 , -0.09 ] |
| 2 | Intercept | Lexical Fluency | -0.08 [ -0.19 , -0.01 ] |
| | | Semantic Fluency | -0.12 [ -0.23 , -0.06 ] |
| | | Short Term Memory | -0.15 [ -0.24 , -0.08 ] |
| | Slope | Lexical Fluency | 0.13 [ 0.07 , 0.24 ] |
| | | Semantic Fluency | 0.15 [ 0.09 , 0.26 ] |
| | | Inductive Reasoning | 0.14 [ 0.08 , 0.25 ] |
| | | Verbal Reasoning | 0.1 [ 0.04 , 0.22 ] |
| | | Mathematical Reasoning | 0.13 [ 0.09 , 0.25 ] |

## 3.4 Brain-Cognition Latent Variables Predict Cognitive Performance at Future Timepoint

To investigate the biological significance of the brain-cognition relationships identified by the two distinct LVs, we assessed how expression of LVs predicted cognitive performance at a future time point (Wave 12, 2015-16, on average 3.2 years post MRI collection). Within each LV, a behavior score was computed for each subject. For example, a subject with a positive LV1 behavior score would express the LV1 cognitive phenotype, whereas a subject with a negative LV1 behavior score would express the inverse cognitive pattern (Figure 4A).

Higher expression of the LV1 phenotype was associated with having fewer years of education ($\beta$=-0.43, $p<0.01$) and lower MOCA scores (i.e. greater cognitive impairment) ($t(98.5)=7.9$, $p<0.01$, Figure 4B) at the Imaging Wave. However, LV2 scores were not related to either MOCA ($t(101.9)=0.79$, $p>0.05$) or education ($\beta$=-0.04, $p>0.05$) (Figure 4B). Both LV1 and LV2 showed sex differences, with females having higher LV1 but lower LV2 scores in comparison to males (SI Results and Figure S3). Neither LV1 or LV2 showed any relationship to age (SI Results and Figure S3).

We next performed linear models to examine the relationship between LV scores and Wave 12 cognitive performance. Table 3 lists unstandardized coefficients and p values of these analyses, assessing significance at Bonferroni corrected threshold of $0<0.0083$ (0.05/6) . We observed that high expression of LV1 scores was associated with lower performance on each test. Conversely, higher expression of the LV2 was associated with lower Wave 12 performance of semantic fluency, lexical fluency, and memory tests but better performance on inductive, mathematical, and verbal reasoning tests. Thus, we find both LV1 and LV2 are predictive of future cognitive performance in unique and distinct ways.

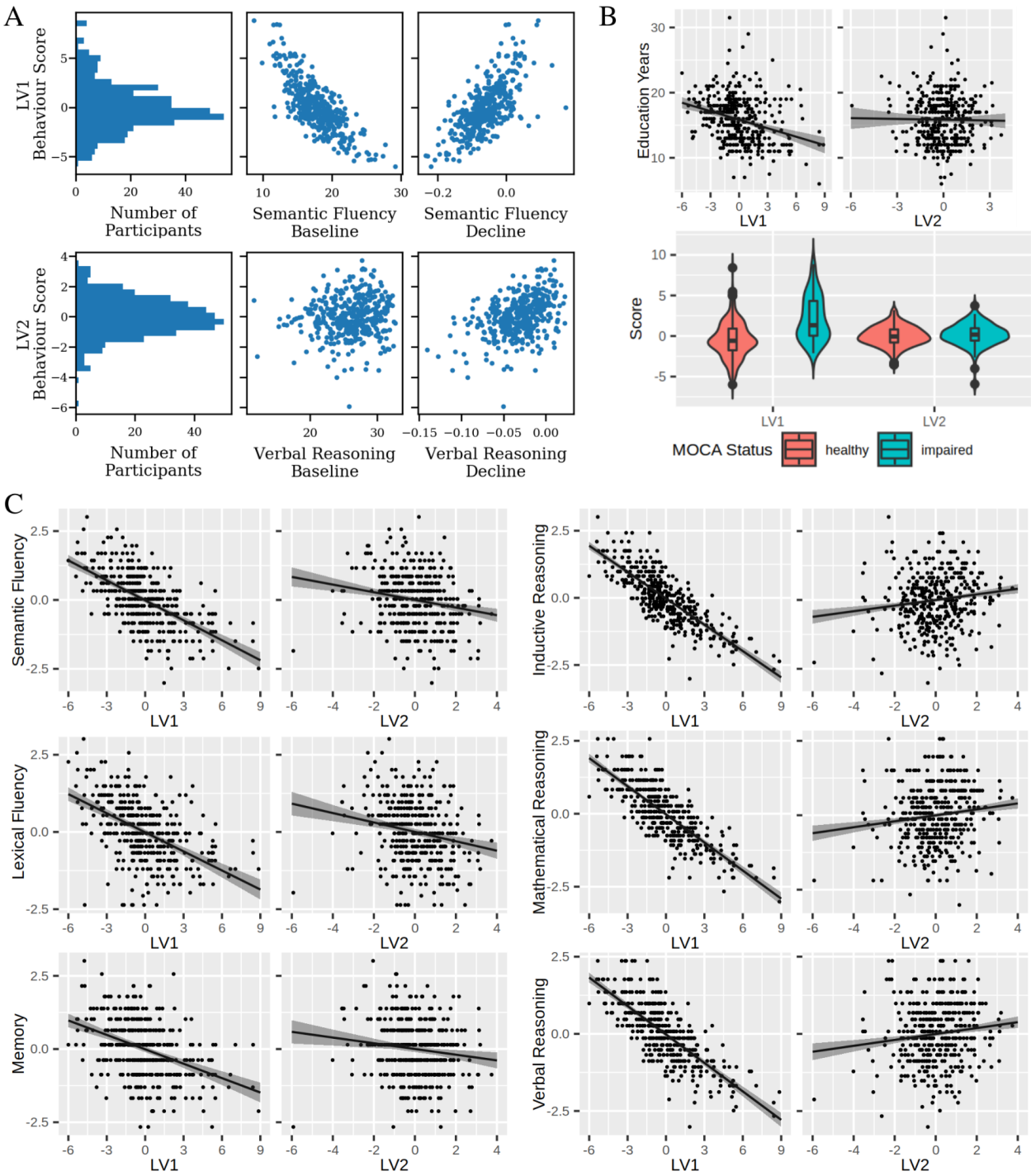


Figure 4: **Individual expression of PLS derived brain-cognition latent variables is indicative of cognitive status and future performance**. We used each subject's expression of LV1 and LV2 to predict their cognitive performance at a future wave (Wave 12, 3.2 years post Imaging Wave, on average). A) An illustration of the utility of LV behavior scores. Top row: a histogram shows the distribution of LV1 behavior scores, which quantify the degree to which each subject expresses the phenotype described by LV1. Plots of LV1 versus semantic fluency baseline and decline measures show positive and negative relationships, respectively. These match that described in LV1 in

Figure 3, demonstrating that LV behavior scores can be used to describe the cognitive phenotype of subjects. Bottom row: equivalent plots for LV2 including the histogram, and plots of LV2 behavior scores vs verbal reasoning baseline (no relation) and verbal reasoning decline (positive relation). B) LV1, but not LV2, behaviour scores relate to key demographic variables. Linear modelling of years of education as a function of LV scores showed a negative relationship with LV1 ($\beta$ = -0.43, $p<0.01$), but no relationship with LV2 ($\beta$ = -0.04, $p>0.05$). Similarly, t-test of mean score between healthy and impaired MOCA groups showed significant differences for LV1 ($t(98.5)=7.9$, $p<0.01$) but not LV2 ($t(101.9)=0.79$, $p>0.05$). C) Effects plots of each Wave 12 test vs. LV1 and LV2, respectively. Effects plots, created using the effects() R function, plot the predicted test score at various levels of either LV1 or LV2 while assuming population averages for other covariates. Shaded areas represent confidence intervals around the estimate. Table 3 displays statistics from the linear models used to assess these relationships, each of which was significant at a bonferroni threshold of $p < 0.0083$ (0.05/6).

**Table 3:** Statistical results from linear models run for Wave 12 performance on each of 6 cognitive tests. Each model had the form $Test \sim LV1 + LV2 + Age + Sex + Education$. Unstandardized beta coefficients and 95% confidence intervals are reported. Bolded p values are deemed significant at a bonferroni threshold of $p<0.0083$.

| Test | Term | β [95% CI] | p |
|---|---|---|---|
| Semantic Fluency | LV1 | -0.24 [-0.27 -0.21] | **<0.001** |
| | LV2 | -0.14 [-0.20 -0.08] | **<0.001** |
| Lexical Fluency | LV1 | -0.21 [-0.24 -0.17] | **<0.001** |
| | LV2 | -0.15 [-0.21 0.09] | **<0.001** |
| Memory | LV1 | -0.16 [-0.2 -0.14] | **<0.001** |
| | LV2 | -0.1 [-0.16 -0.03] | **0.003** |
| Inductive Reasoning | LV1 | -0.33 [-0.35 -0.3] | **<0.001** |
| | LV2 | 0.1 [0.06 0.14] | **<0.001** |
| Mathematical Reasoning | LV1 | -0.32 [-0.34 -0.3] | **<0.001** |
| | LV2 | 0.1 [0.06 0.14] | **<0.001** |
| Verbal Reasoning | LV1 | -0.31 [-0.33 -0.28] | **<0.001** |
| | LV2 | 0.1 [0.05 0.14] | **<0.001** |

# 4.0 Discussion

In this study, we used a data-driven approach to identify brain-cognition latent variables of covariance linking individual variation in cognitive decline over a period of 20-years from mid-to-late life, with later-life patterns of cortical microstructure. We present several novel results. We identified 10 microstructural components which integrate multimodal MRI data to take advantage of the complementary information conveyed by these indices of cortical microstructure. First, we describe two distinct brain-cognition latent variables that describe covariance between longitudinal cognitive

performance and cortical microstructure. Notably, these LVs do not describe a homogenous or directionally uniform link between cognitive decline and degeneration of cortical microstructure. By avoiding broad categorisations of cognitive maintainers or decliners, these LVs instead describe a more complex pattern of intra-and inter-individual variability, whereby individuals presented a mixed distribution of 20-year cognitive decline *and* maintenance which were associated with both degeneration *and* preservation of cortical microstructure in older age. Second, the simultaneous analysis of multimodal MRI measures of brain microstructure better enables us to discuss and understand the neurobiological underpinnings of the identified brain-cognition relationships, especially given the inter-dependency between morphological measures. Third, we show that individual variation within these LVs is predictive of future cognitive performance, helping to understand the biological significance of these distinct brain-cognition LVs. Together, this suggests that the primary determinant of late-life cognitive performance is mid-life cognitive performance and an associated microstructural pattern dominated by cortical surface area.

## 4.1 Brain-Cognition latent variables include a mixture of maintenance and decline

The two brain-cognition relationships identified in this work contain a mixture of positive and negative features across both brain and cognition. The first brain-cognition LV describes a pattern of low midlife performance across all tests, accelerated decline in reasoning, but relatively maintained fluency associated with a multimodal pattern of low SA in all areas of the brain except for the primary and supplementary motor cortices, decreased CT in cingulate and insular cortex, increased diffusivity in the temporal pole, decreased FA in visual, temporal, and right lateral cortex but increased FA in superior frontal and lateral temporal regions. Meanwhile, the second brain-cognition LV links low baseline fluency and memory performance, but slower fluency and reasoning declines with increased diffusivities in nearly all regions except occipital cortex, increased surface area in cingulate, insular and right lateral areas, increased temporal pole thickness, and decreased FA in frontal, cingulate and insular regions. Thus, across both brain and cognition, we observe a mix of what studies have traditionally characterised as adaptive and maladaptive characteristics. While it may be tempting to infer patterns of overall cognitive or neuroanatomical maintenance, our work suggests that by refraining from *a priori* definitions of maintenance or decline groups, including baseline and decline measures across a range of tests, and analysing multimodal indices of cortical microstructure simultaneously, we can identify subtle, complex brain-cognition relationships which show a mix of maintenance and decline features across both cognitive and anatomical measures. These findings thus discourage the use of a ‘one size fits all’ approach, and instead encourage the consideration of cognitive domains and regional, multivariate anatomy at the individual level.

While we cannot derive direct mechanistic inferences, our results also shed light on the neurobiological underpinnings of the two latent variables. Histological evidence links CT reductions in old age with decreased dendritic arborization (Esiri 2007; Goriounova et al. 2018). A recent application of virtual histology supports this, having found cortical thinning is related to increased expression of CA1 pyramidal cell gene sets enriched with processes related to dendritic arborization approach correlated

longitudinal CT changes with cell type expression levels (Vidal-Pineiro et al. 2020; Patel et al. 2021). Corresponding studies of SA remain uninvestigated, though see our discussion in Section 3.2 for more on our SA findings. DWI metrics may relate to a range of age-related alterations as decline in small diameter myelinated fibers, alterations in the myelin sheath, and inflammatory processes (Beaulieu 2002; Marner et al. 2003). Increased diffusivity is a common finding in aging studies, and may relate to enlarged interstitial spaces or axon swelling (Benedetti et al. 2006; Madden et al. 2012; Chad et al. 2018). Rodent studies incorporating imaging and histology demonstrate that demyelination of axons leads to increased RD (Song et al. 2002, 2004; Sun et al. 2008; Tuor et al. 2014), while reductions in FA relate to degradation of structure and preferential orientation of fibers (Alexander et al. 2007; Tuor et al. 2014). We hypothesize that LV1 has a neurobiological pattern of widespread reductions in cortical area, dendritic branching, demyelination, and axonal degeneration while LV2 is associated with near global demyelination and axonal degeneration, but relatively maintained cortical area in cingulate, insular, right lateral cortex and dendritic morphology in the temporal pole. However, while plausible, these interpretations are complicated by the fact that each MRI metric is sensitive to a large range of cellular level alterations (Zatorre et al. 2012; Tardif et al. 2016) as well as the interrelated nature of the DWI metrics analysed (Madden et al. 2012). While joint analyses of all metrics, as is a focus of this work, may help alleviate some concerns (Assaf and Pasternak 2008), caution is still warranted in absence of direct histological evidence.

## 4.2 Late Life Cognitive Performance is Driven by Mid Life Phenotypes

In our study sample and within the timeframe examined, the strongest predictor of later life (>65 years) cognitive performance across a range of tests was performance in midlife (at mean age of 40 years). We assessed the relationship between LV behaviour scores and cognitive performance at a future timepoint and found that across all tests, individuals scoring high on LV1 performed worse than those who expressed the inverse cognitive pattern. In certain cases this is a straightforward result, as the cognition features of LV1 included either decreased baseline performance (memory) or both decreased baseline performance and accelerated decline (inductive, mathematical, and verbal reasoning). However, for tests of lexical and semantic fluency LV1 describes low baseline performance and slower decline. In this case, the inverse relationship between LV1 and future performance shows the relative maintenance of these abilities is not enough to compensate for lower initial performance. Individuals scoring high on LV2 performed worse on tests of fluency and memory, but better on tests of inductive, mathematical, and verbal reasoning compared to those with lower LV2 scores. Similar to LV1, LV2 describes low baseline performance and slower decline on both fluency measures, and the inverse relationship between LV2 and future performance shows maintenance is not enough to compensate for lower initial performance. For tests of inductive, verbal and mathematical reasoning, LV2 describes a relative maintenance without any baseline effects, in line with the positive association between LV2 and future performance on these tests.

Inclusion of both LV1 and LV2 scores in our models suggests that each of the brain-cognition LVs identified are distinct in their ability to predict future cognitive performance. That we covaried for impacts of age, sex, and education further supports the unique impact of each LV, over and above other factors considered. For tests of inductive, mathematical, and verbal reasoning, LV1 and LV2 describe opposing characteristics with LV1 showing low baseline performance and accelerated decline and LV2

showing a relative maintenance over time. When predicting future performance, we found that LV1 beta coefficients were consistently larger in magnitude compared to LV2, suggesting the low midlife characteristics of LV1 have a larger impact on future performance than the maintenance characteristics of LV2. This supports the notion that low midlife performance is not adequately countered by the identified longitudinal maintenance. This finding has relevance to the concept of cognitive reserve. High levels of cognitive reserve, often probed through proxies such as education or occupational attainment, have been strongly linked to better cognitive function in aging (Ewers 2020). Whether this is driven by a maintenance of previously developed advantages, moderation of the effects of aging on cognition and hence cognitive decline, or a combination however remains unclear (Ewers 2020; Soldan et al. 2020). Our findings altogether suggest that midlife differences in cognitive performance were the most prominent predictors. However, it may be that individuals in our study sample have not yet reached a point of drastically accelerated decline and therefore showed relatively less profound differences in cognitive trajectories (Gregory et al. 2017).

While the MRI data is cross sectional and collected only in late life, in the context of mid life dominance we find the widespread involvement of SA to be of particular interest. SA is commonly assessed in parallel with CT, though the contribution of each to cortical volume, as well as their neurobiological and genetic underpinnings (Rakic 1988, 2000; Panizzon et al. 2009; Storsve et al. 2014), varies. For example, while each of SA, CT, and cortical volume decrease with age, CT and volume change are positively correlated while changes between CT and SA tend to be inversely related (Storsve et al. 2014). SA decreases during aging are also of smaller magnitude than those observed for CT (Storsve et al. 2014), and the primary determinant of SA, cortical column generation, occurs during prenatal and perinatal periods (Rakic 1988, 2000). These findings suggest SA may be more temporally fixed than CT between mid and late life, and throughout the full lifespan. In this context, the pronounced influence of LV1 mid life cognitive performance and late life SA on late life cognition lends credence to a lifespan perspective in which developmental and mid-life events play a significant role in cognitive health in late life. In a unique study involving the Lothian Birth Cohort, positive cognitive ageing between childhood (age 11) and late life (age 73) was associated with higher SA in late life (Cox et al. 2018). In another unique study involving multiple samples, Walhovd et al. identified a large region of the cortex in which increased general cognitive ability was associated with increased surface area in a developmental sample (aged 4-12) and noted that this association persisted throughout the lifespan (Walhovd et al. 2016). Our findings, along with others, support the idea that stable advantages may give certain individuals a 'head start' in terms of cognitive function in aging. They also support the need for early and mid-life preventative measures of cognitive decline to maintain cognitive performance in older ages, though the potential role of reserve mechanisms on cognitive decline warrant further investigation. The mixed, complex relationships identified also support the development of individualized preventative strategies. Interestingly, within a subset of the Whitehall II cohort, previous work has identified similar mid to late life relationships across different biological domains such that midlife cardiovascular health was predictive of indicative of cerebral hypoperfusion in late life (Suri et al. 2019).

## 4.3 Strengths and Limitations

A key strength of this study is the use of multimodal MRI data to characterize cortical morphology. Use of multiple MRI metrics provides complementary information regarding anatomical properties of the brain in comparison to unimodal analyses. We take this further by employing NMF to analyse multimodal data simultaneously to capture shared patterns of covariance across measures. This approach allows us to identify 10 major components which are spatially contiguous and highlight relevant regions in which cortical morphology varies across subjects. We relate this variability to longitudinal cognitive performance using PLS. This approach does not limit us to broad categorizations of decliners or maintainers, rather, we obtain continuous measures for each individual identifying the degree of expression of each of the identified brain-cognition latent variables. The use of multimodal data and longitudinal cognitive measures is made possible by the unique dataset analysed. However, our study is limited by a smaller sample size in comparison to large scale neuroimaging analyses. It may be that more brain-cognition relationships would be identifiable in a larger sample. Our study also lacks an out of sample validation, as the unique longitudinal data makes a compatible out of sample dataset difficult to find. In addition to this, the Whitehall II Imaging Sub-study cohort contains a higher proportion of men compared to the general population and is relatively more educated. Thus, generalizability of our findings to the wider population is limited. While we were able to quantify 20-year cognitive trajectories, MRI data is currently available at a single time-point which limits investigations of longitudinal brain-cognition relationships. Furthermore, while a combination of structural and diffusion MRI was used to provide a more comprehensive assessment of cortical microstructure, the limitations of MRI, in particular its resolution in comparison to the neural substrates under study, preclude us from inferring the cellular mechanisms which may be at play (Tardif et al. 2017).

# 5.0 Conclusion

This work provides novel information on brain-cognition relationships in a healthy elderly population. We uncover complex brain-cognition relationships using an unbiased data-driven approach, free of a priori definitions of cognitive maintainers or decliners and including a rich and comprehensive longitudinal cognitive data and multimodal MRI measures. This supports future works including multimodal data as well as cognitive trajectories to capture the full range of brain-cognition relationships. We also find the largest determinant of late life cognition is mid life cognition, as opposed to the rate of decline over time. This, and the associated link with widespread surface area measurements, support early and mid-life preventative measures of cognitive decline.

# Funding

This research was funded in whole, or in part, by the Wellcome Trust [Grant number 203139/Z/16/Z]. For the purpose of open access, the author has applied a CC BY public copyright licence to any Author Accepted Manuscript version arising from this submission.

The Whitehall II study is supported by the British Heart Foundation (RG/16/11/32334), UK Medical Research Council (K013351) and US National Institute on Aging (R01AG056477; RF1AG062553). The Whitehall II Imaging Sub-study was supported by the UK Medical Research Council (MRC) grants "Predicting MRI abnormalities with longitudinal data of the Whitehall II Sub-study" (G1001354; PI KPE; ClinicalTrials.gov Identifier: NCT03335696), and "Adult Determinants of Late Life Depression, Cognitive Decline and Physical Functioning - The Whitehall II Ageing Study" (MR/K013351/1; PI: MK). Working on this study was also supported by European Commission (Horizon 2020 grant "Lifebrain", 732592; co-PI KPE), the HDH Wills 1965 Charitable Trust (1117747; PI KPE) and the UK National Institute of Health Research (NIHR) Oxford Health Biomedical Research Centre (BRC). The Wellcome Centre for Integrative Neuroimaging (WIN) is supported by core funding from the Wellcome Trust (203139/Z/16/Z). **RP** is funded through the Fonds de Recherche du Quebec - Santé (Doctoral Training). **SS** is funded through Alzheimer's Society Research Fellowship (Grant Number 441), **KPE** through UK Medical Research Council (G1001354, MR/K013351/), HDH Wills 1965 Charitable Trust (1117747), Alzheimer Research UK (PPG2012A-5) and the European Commission (Horizon 2020 grant "Lifebrain", 732592), **EZs** UK Medical Research Council (G1001354, MR/K013351/), HDH Wills 1965 Charitable Trust (1117747), Horizon 2020 grant "Lifebrain", 732592; co-PI KPE), **MK** through UK MRC (MR/K013351/1, MR/R024227/1, MR/S011676/1), National Institute on Aging (NIH), US (R01AG056477), NordForsk (75021), Academy of Finland (311492), Helsinki Institute of Life Science Fellowship (H970), **ASM** through NIH (R01AG056477, R01AG062553).

Work on this study received institutional support from the UK National Institute of Health Research (NIHR) Oxford Health Biomedical Research Centre (BRC) and the Wellcome Centre for Integrative Neuroimaging (WIN). The WIN is supported by core funding from the Wellcome Trust (203139/Z/16/Z).

The views expressed are those of the authors and not necessarily those of the NHS, the NIHR or the Department of Health.

# Acknowledgements

We would like to thank all contributors to the Whitehall II study. We thank all the participating civil service departments; the British Occupational Health and Safety Agency; the British Council of Civil Service Unions; all participating civil servants in the Whitehall II Study; and all members of the Whitehall II Study team at University College London who so helpfully collaborated with us. The Whitehall II Study team comprises research scientists, statisticians, study coordinators, nurses, data managers, administrative assistants, and data entry staff, who make the study possible. We would like to

thank staff at the Wellcome Centre for Integrative Neuroimaging in Oxford who acquired scans, in particular Dr Nicola Filippini (DPhil) and research radiographers Michael Sanders, MSc, Jon Campbell, MMRTech, BcAppSc, Caroline Young, DCR(R), David Parker, BSc(Hons). Martin R. Turner, MA, MBBS, PhD, FRCP (Wellcome Centre for Integrative Neuroimaging, Oxford, United Kingdom), and his colleagues advised on incidental findings and taking over clinical responsibility for such participants.

# References


Ad-Dab'bagh Y, Lyttelton O, Muehlboeck JS, Lepage C, Einarson D, Mok K, Ivanov O, Vincent RD, Lerch J, Fombonne E, Others. 2006. The CIVET image-processing environment: a fully automated comprehensive pipeline for anatomical neuroimaging research. In: Proceedings of the 12th annual meeting of the organization for human brain mapping. Florence, Italy.

Alexander AL, Lee JE, Lazar M, Field AS. 2007. Diffusion tensor imaging of the brain. Neurotherapeutics. 4:316–329.

Assaf Y, Pasternak O. 2008. Diffusion tensor imaging (DTI)-based white matter mapping in brain research: a review. J Mol Neurosci. 34:51–61.

Bartzokis G. 2004. Age-related myelin breakdown: a developmental model of cognitive decline and Alzheimer's disease. Neurobiol Aging. 25:5–18.

Beaulieu C. 2002. The basis of anisotropic water diffusion in the nervous system--a technical review. NMR Biomed. 15:435–455.

Benedetti B, Charil A, Rovaris M, Judica E, Valsasina P, Sormani MP, Filippi M. 2006. Influence of aging on brain gray and white matter changes assessed by conventional, MT, and DT MRI. Neurology. 66:535–539.

Boutsidis C, Gallopoulos E. 2008. SVD based initialization: A head start for nonnegative matrix factorization. Pattern Recognit. 41:1350–1362.

Chad JA, Pasternak O, Salat DH, Chen JJ. 2018. Re-examining age-related differences in white matter microstructure with free-water corrected diffusion tensor imaging. Neurobiol Aging. 71:161–170.

Cox SR, Bastin ME, Ritchie SJ, Dickie DA, Liewald DC, Muñoz Maniega S, Redmond P, Royle NA, Pattie A, Valdés Hernández M, Corley J, Aribisala BS, McIntosh AM, Wardlaw JM, Deary IJ. 2018. Brain cortical characteristics of lifetime cognitive ageing. Brain Struct Funct. 223:509–518.

De Jager PL, Shulman JM, Chibnik LB, Keenan BT, Raj T, Wilson RS, Yu L, Leurgans SE, Tran D, Aubin C, Anderson CD, Biffi A, Corneveaux JJ, Huentelman MJ, Alzheimer's Disease Neuroimaging Initiative, Rosand J, Daly MJ, Myers AJ, Reiman EM, Bennett DA, Evans DA. 2012. A genome-wide scan for common variants affecting the rate of age-related cognitive decline. Neurobiol Aging. 33:1017.e1–e15.

Esiri MM. 2007. Ageing and the brain. J Pathol. 211:181–187.

Eskildsen SF, Coupé P, Fonov V, Manjón JV, Leung KK, Guizard N, Wassef SN, Østergaard LR, Collins DL, Alzheimer's Disease Neuroimaging Initiative. 2012. BEaST: brain extraction based on nonlocal segmentation technique. Neuroimage. 59:2362–2373.

Ewers M. 2020. Reserve in Alzheimer's disease: update on the concept, functional mechanisms and sex differences. Curr Opin Psychiatry. 33:178–184.

Filippini N, Zsoldos E, Haapakoski R, Sexton CE, Mahmood A, Allan CL, Topiwala A, Valkanova V, Brunner EJ, Shipley MJ, Auerbach E, Moeller S, Uğurbil K, Xu J, Yacoub E, Andersson J, Bijsterbosch J, Clare S, Griffanti L, Hess AT, Jenkinson M, Miller KL, Salimi-Khorshidi G, Sotiropoulos SN, Voets NL, Smith SM, Geddes JR, Singh-Manoux A, Mackay CE, Kivimäki M, Ebmeier KP. 2014. Study protocol: The Whitehall II imaging sub-study. BMC Psychiatry. 14:159.

Fjell AM, McEvoy L, Holland D, Dale AM, Walhovd KB, Alzheimer's Disease Neuroimaging Initiative. 2014. What is normal in normal aging? Effects of aging, amyloid and Alzheimer's disease on the cerebral cortex and the hippocampus. Prog Neurobiol. 117:20–40.

Glasser MF, Coalson TS, Robinson EC, Hacker CD, Harwell J, Yacoub E, Ugurbil K, Andersson J, Beckmann CF, Jenkinson M, Smith SM, Van Essen DC. 2016. A multi-modal parcellation of human

cerebral cortex. Nature. 536:171–178.
Goh JO, An Y, Resnick SM. 2012. Differential trajectories of age-related changes in components of executive and memory processes. Psychol Aging. 27:707–719.
Goriounova NA, Heyer DB, Wilbers R, Verhoog MB, Giugliano M, Verbist C, Obermayer J, Kerkhofs A, Smeding H, Verberne M, Idema S, Baayen JC, Pieneman AW, de Kock CP, Klein M, Mansvelder HD. 2018. Large and fast human pyramidal neurons associate with intelligence. Elife. 7.
Gregory S, Long JD, Klöppel S, Razi A, Scheller E, Minkova L, Papoutsi M, Mills JA, Durr A, Leavitt BR, Roos RAC, Stout JC, Scahill RI, Langbehn DR, Tabrizi SJ, Rees G. 2017. Operationalizing compensation over time in neurodegenerative disease. Brain. 140:1158–1165.
Groves AR, Smith SM, Fjell AM, Tamnes CK, Walhovd KB, Douaud G, Woolrich MW, Westlye LT. 2012. Benefits of multi-modal fusion analysis on a large-scale dataset: life-span patterns of inter-subject variability in cortical morphometry and white matter microstructure. Neuroimage. 63:365–380.
Hedman AM, van Haren NEM, Schnack HG, Kahn RS, Hulshoff Pol HE. 2012. Human brain changes across the life span: a review of 56 longitudinal magnetic resonance imaging studies. Hum Brain Mapp. 33:1987–2002.
Heim AW. 1970. Manual for the AH4 group test of general intelligence. Windsor: NFER.
Josefsson M, de Luna X, Pudas S, Nilsson L-G, Nyberg L. 2012. Genetic and lifestyle predictors of 15-year longitudinal change in episodic memory. J Am Geriatr Soc. 60:2308–2312.
Krishnan A, Williams LJ, McIntosh AR, Abdi H. 2011. Partial Least Squares (PLS) methods for neuroimaging: a tutorial and review. Neuroimage. 56:455–475.
Lebel C, Gee M, Camicioli R, Wieler M, Martin W, Beaulieu C. 2012. Diffusion tensor imaging of white matter tract evolution over the lifespan. Neuroimage. 60:340–352.
Lee DD, Seung HS. 1999. Learning the parts of objects by non-negative matrix factorization. Nature. 401:788–791.
Lerch JP, Evans AC. 2005. Cortical thickness analysis examined through power analysis and a population simulation. Neuroimage. 24:163–173.
Lerch JP, van der Kouwe AJW, Raznahan A, Paus T, Johansen-Berg H, Miller KL, Smith SM, Fischl B, Sotiropoulos SN. 2017. Studying neuroanatomy using MRI. Nat Neurosci. 20:314–326.
Lowe AJ, Paquola C, Vos de Wael R, Girn M, Lariviere S, Tavakol S, Caldairou B, Royer J, Schrader DV, Bernasconi A, Bernasconi N, Spreng RN, Bernhardt BC. 2019. Targeting age-related differences in brain and cognition with multimodal imaging and connectome topography profiling. Hum Brain Mapp. 40:5213–5230.
Madden DJ, Bennett IJ, Burzynska A, Potter GG, Chen N-K, Song AW. 2012. Diffusion tensor imaging of cerebral white matter integrity in cognitive aging. Biochim Biophys Acta. 1822:386–400.
Manjón JV, Coupé P, Martí-Bonmatí L, Collins DL, Robles M. 2010. Adaptive non-local means denoising of MR images with spatially varying noise levels. J Magn Reson Imaging. 31:192–203.
Marmot M, Brunner E. 2005. Cohort Profile: the Whitehall II study. Int J Epidemiol. 34:251–256.
Marner L, Nyengaard JR, Tang Y, Pakkenberg B. 2003. Marked loss of myelinated nerve fibers in the human brain with age. J Comp Neurol. 462:144–152.
McIntosh AR, Lobaugh NJ. 2004. Partial least squares analysis of neuroimaging data: applications and advances. Neuroimage. 23 Suppl 1:S250–S263.
McIntosh AR, Mišić B. 2013. Multivariate statistical analyses for neuroimaging data. Annu Rev Psychol. 64:499–525.
Nordin K, Persson J, Stening E, Herlitz A, Larsson E-M, Söderlund H. 2018. Structural whole-brain covariance of the anterior and posterior hippocampus: Associations with age and memory. Hippocampus. 28:151–163.
Panizzon MS, Fennema-Notestine C, Eyler LT, Jernigan TL, Prom-Wormley E, Neale M, Jacobson K,

Lyons MJ, Grant MD, Franz CE, Xian H, Tsuang M, Fischl B, Seidman L, Dale A, Kremen WS. 2009. Distinct genetic influences on cortical surface area and cortical thickness. Cereb Cortex. 19:2728–2735.
Park DC, Reuter-Lorenz P. 2009. The Adaptive Brain: Aging and Neurocognitive Scaffolding. Annu Rev Psychol. 60:173–196.
Patel R, Steele CJ, Chen AGX, Patel S, Devenyi GA, Germann J, Tardif CL, Chakravarty MM. 2020. Investigating microstructural variation in the human hippocampus using non-negative matrix factorization. Neuroimage. 207:116348.
Patel Y, Parker N, Shin J, Howard D, French L, Thomopoulos SI, Pozzi E, Abe Y, Abé C, Anticevic A, Others. 2021. Virtual histology of cortical thickness and shared neurobiology in 6 psychiatric disorders. JAMA Psychiatry. 78:47–63.
Persson J, Nyberg L, Lind J, Larsson A, Nilsson L-G, Ingvar M, Buckner RL. 2006. Structure-function correlates of cognitive decline in aging. Cereb Cortex. 16:907–915.
Persson J, Pudas S, Lind J, Kauppi K, Nilsson L-G, Nyberg L. 2012. Longitudinal structure-function correlates in elderly reveal MTL dysfunction with cognitive decline. Cereb Cortex. 22:2297–2304.
Philippi N, Noblet V, Duron E, Cretin B, Boully C, Wisniewski I, Seux ML, Martin-Hunyadi C, Chaussade E, Demuynck C, Kremer S, Lehéricy S, Gounot D, Armspach JP, Hanon O, Blanc F. 2016. Exploring anterograde memory: a volumetric MRI study in patients with mild cognitive impairment. Alzheimers Res Ther. 8:26.
Pudas S, Persson J, Josefsson M, de Luna X, Nilsson L-G, Nyberg L. 2013. Brain characteristics of individuals resisting age-related cognitive decline over two decades. J Neurosci. 33:8668–8677.
Rakic P. 1988. Specification of cerebral cortical areas. Science. 241:170–176.
Rakic P. 2000. Radial unit hypothesis of neocortical expansion. Novartis Found Symp. 228:30–42; discussion 42–52.
Raven JC. 1958. Guide to using the Mill Hill Vocabulary Scale with the Progressive Matrices Scales. 64.
Raz N, Rodrigue KM. 2006. Differential aging of the brain: Patterns, cognitive correlates and modifiers. Neurosci Biobehav Rev. 30:730–748.
Reas ET, Hagler DJ Jr, White NS, Kuperman JM, Bartsch H, Wierenga CE, Galasko D, Brewer JB, Dale AM, McEvoy LK. 2018. Microstructural brain changes track cognitive decline in mild cognitive impairment. Neuroimage Clin. 20:883–891.
Rönnlund M, Nyberg L, Bäckman L, Nilsson L-G. 2005. Stability, growth, and decline in adult life span development of declarative memory: cross-sectional and longitudinal data from a population-based study. Psychol Aging. 20:3–18.
Salthouse T. 2010. Selective review of cognitive aging. Journal of International Neuropsychology. 16:754–760.
Schneider ALC, Senjem ML, Wu A, Gross A, Knopman DS, Gunter JL, Schwarz CG, Mosley TH, Gottesman RF, Sharrett AR, Jack CR Jr. 2019. Neural correlates of domain-specific cognitive decline: The ARIC-NCS Study. Neurology. 92:e1051–e1063.
Seidlitz J, Váša F, Shinn M, Romero-Garcia R, Whitaker KJ, Vértes PE, Wagstyl K, Kirkpatrick Reardon P, Clasen L, Liu S, Messinger A, Leopold DA, Fonagy P, Dolan RJ, Jones PB, Goodyer IM, NSPN Consortium, Raznahan A, Bullmore ET. 2018. Morphometric Similarity Networks Detect Microscale Cortical Organization and Predict Inter-Individual Cognitive Variation. Neuron. 97:231–247.e7.
Shaw ME, Sachdev PS, Anstey KJ, Cherbuin N. 2016. Age-related cortical thinning in cognitively healthy individuals in their 60s: the PATH Through Life study. Neurobiol Aging. 39:202–209.
Singh-Manoux A, Kivimaki M, Glymour MM, Elbaz A, Berr C, Ebmeier KP, Ferrie JE, Dugravot A. 2012. Timing of onset of cognitive decline: results from Whitehall II prospective cohort study. BMJ. 344:d7622.
Soldan A, Pettigrew C, Albert M. 2020. Cognitive Reserve from the Perspective of Preclinical Alzheimer

Disease: 2020 Update. Clin Geriatr Med. 36:247–263.
Song S-K, Kim JH, Lin S-J, Brendza RP, Holtzman DM. 2004. Diffusion tensor imaging detects age-dependent white matter changes in a transgenic mouse model with amyloid deposition. Neurobiol Dis. 15:640–647.
Song S-K, Sun S-W, Ramsbottom MJ, Chang C, Russell J, Cross AH. 2002. Dysmyelination revealed through MRI as increased radial (but unchanged axial) diffusion of water. Neuroimage. 17:1429–1436.
Sotiras A, Resnick SM, Davatzikos C. 2015. Finding imaging patterns of structural covariance via Non-Negative Matrix Factorization. Neuroimage. 108:1–16.
Stern Y, Arenaza‐Urquijo EM, Bartrés‐Faz D, Belleville S, Cantilon M, Chetelat G, Ewers M, Franzmeier N, Kempermann G, Kremen WS, Okonkwo O, Scarmeas N, Soldan A, Udeh‐Momoh C, Valenzuela M, Vemuri P, Vuoksimaa E, and the Reserve, Resilience and Protective Factors PIA Empirical Definitions and Conceptual Frameworks Workgroup. 2020. Whitepaper: Defining and investigating cognitive reserve, brain reserve, and brain maintenance. Alzheimer's & Dementia.
Storsve AB, Fjell AM, Tamnes CK, Westlye LT, Overbye K, Aasland HW, Walhovd KB. 2014. Differential longitudinal changes in cortical thickness, surface area and volume across the adult life span: regions of accelerating and decelerating change. J Neurosci. 34:8488–8498.
Sun S-W, Liang H-F, Cross AH, Song S-K. 2008. Evolving Wallerian degeneration after transient retinal ischemia in mice characterized by diffusion tensor imaging. Neuroimage. 40:1–10.
Suri S, Topiwala A, Chappell MA, Okell TW, Zsoldos E, Singh-Manoux A, Kivimäki M, Mackay CE, Ebmeier KP. 2019. Association of Midlife Cardiovascular Risk Profiles With Cerebral Perfusion at Older Ages. JAMA Netw Open. 2:e195776.
Tardif CL, Gauthier CJ, Steele CJ, Bazin P-L, Schäfer A, Schaefer A, Turner R, Villringer A. 2016. Advanced MRI techniques to improve our understanding of experience-induced neuroplasticity. Neuroimage. 131:55–72.
Tardif CL, Steele CJ, Lampe L, Bazin P-L, Ragert P, Villringer A, Gauthier CJ. 2017. Investigation of the confounding effects of vasculature and metabolism on computational anatomy studies. Neuroimage. 149:233–243.
Tucker-Drob EM. 2011a. Neurocognitive functions and everyday functions change together in old age. Neuropsychology. 25:368–377.
Tucker-Drob EM. 2011b. Global and domain-specific changes in cognition throughout adulthood. Dev Psychol. 47:331–343.
Tucker-Drob EM, Salthouse TA. 2011. Individual Differences in Cognitive Aging. In: Chamorro-Premuzic T,, von Stumm S,, Furnham A, editors. The Wiley-Blackwell Handbook of Individual Differences. Oxford, UK: Wiley-Blackwell. p. 242–267.
Tuor UI, Morgunov M, Sule M, Qiao M, Clark D, Rushforth D, Foniok T, Kirton A. 2014. Cellular correlates of longitudinal diffusion tensor imaging of axonal degeneration following hypoxic-ischemic cerebral infarction in neonatal rats. Neuroimage Clin. 6:32–42.
Tustison NJ, Avants BB, Cook PA, Zheng Y, Egan A, Yushkevich PA, Gee JC. 2010. N4ITK: improved N3 bias correction. IEEE Trans Med Imaging. 29:1310–1320.
Vidal-Pineiro D, Parker N, Shin J, French L, Grydeland H, Jackowski AP, Mowinckel AM, Patel Y, Pausova Z, Salum G, Sørensen Ø, Walhovd KB, Paus T, Fjell AM, Alzheimer's Disease Neuroimaging Initiative and the Australian Imaging Biomarkers and Lifestyle flagship study of ageing. 2020. Cellular correlates of cortical thinning throughout the lifespan. Sci Rep. 10:21803.
Walhovd KB, Krogsrud SK, Amlien IK, Bartsch H, Bjørnerud A, Due-Tønnessen P, Grydeland H, Hagler DJ Jr, Håberg AK, Kremen WS, Ferschmann L, Nyberg L, Panizzon MS, Rohani DA, Skranes J, Storsve AB, Sølsnes AE, Tamnes CK, Thompson WK, Reuter C, Dale AM, Fjell AM. 2016. Neurodevelopmental origins of lifespan changes in brain and cognition. Proc Natl Acad Sci U S A.

113:9357–9362.
Wilson RS, Beckett LA, Barnes LL, Schneider JA, Bach J, Evans DA, Bennett DA. 2002. Individual differences in rates of change in cognitive abilities of older persons. Psychol Aging. 17:179–193.
Zatorre RJ, Fields RD, Johansen-Berg H. 2012. Plasticity in gray and white: neuroimaging changes in brain structure during learning. Nat Neurosci. 15:528–536.
Zeighami Y, Fereshtehnejad S-M, Dadar M, Collins DL, Postuma RB, Mišić B, Dagher A. 2017. A clinical-anatomical signature of Parkinson's disease identified with partial least squares and magnetic resonance imaging. Neuroimage.